A Novel Concept in Design of Microwave Planar Dual Band Filter having the Controllable Closed/Isolated Bands by Using the Simple Vias and the Slow Wave Effect for 5G/IoT Applications

Ceyhun Karpuz[#1], Pinar Ozturk Ozdemir[*2], Huriye Senol[#3], Alperen Cengiz [#4], Hasan Huseyin Balik[*5], Adnan Gorur[&6]

[#] Department of Electrical and Electronic Engineering, Pamukkale University, Turkey

[*] Air Force Academy, National Defence University, Turkey

[&] Department of Electrical and Electronic Engineering, Nigde Omer Halisdemir University, Turkey

[1]ckarpuz@pau.edu.tr, [2]oozdemir33@hho.msu.edu.tr, {[3]huriyesenol09, [4]cengizalper118, [5]hasanbalik }@gmail.com, [6]adnangorur@hotmail.com

***Abstract* —A microstrip dual-mode dual-band bandpass filter with slow wave effect is presented in this paper. The slow wave effect is provided by interdigital unit cells. The interdigital unit cell located into microstrip resonator is investigated using full-wave electromagnetic simulations. It is shown that an extra surface area is not required to obtain the slow wave effect using these resonators. Using of metal vias on the resonator allows to be designing a dual-band bandpass filter configuration with out-of-band rejection characteristic. The proposed filter exhibits a wideband frequency response since the I/O ports are directly connected to the resonator. Both simulated and measured results are presented to demonstrate the proposed filter.**

***Keywords* — dual band filter, interdigital unit cell, open circuited stub, slow wave effect.**

I. INTRODUCTION

Miniaturization of microwave components are one of the desirable important requirements in the design of microwave circuits. As is well known from the modern microwave communication system design processes and applications that band-pass/stop filters designed by using microstrip lines are basic structures and have an important place when compared to the other components.

On the other hand, microstrip band-pass filter is a basic structure that has an important place when compared to other microwave circuits. Especially due to the rapid development in wireless communication, dual-band bandpass filters are a great working area. Features such as compact, high performance, high selectivity make microstrip bandpass filters attractive, therefore they are widely used. It is difficult to provide one or more of these features in the filter, and in this regard, various designs can be made. Several methods can be mentioned to obtain dual band filters. A lot of design methodologies for multiband microstrip bandpass filters have been presented by many authors [1-4]. A dual-band bandpass filter using parallel doubly coupled structure with loading capacitance is reported in [1]. It was found that the new

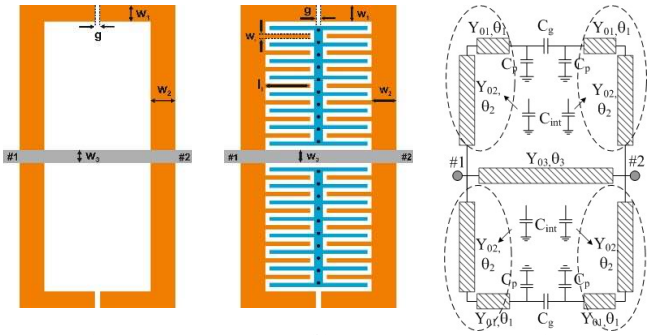

Fig. 1. Layout of resonator (a) without; (b) with interdigital unit cell; (c) equivalent circuit of the proposed resonators.

coupling structure can improve both the layout compactness and performance of the dual band filter. Dual band filters with stepped impedance resonators have been designed due to their dual-band behaviour and simple structure. To obtain a reduced size filter, while a parallel-coupled microstrip dual-band filter using stepped impedance resonators (SIRs) with pleated configuration is presented in [2], a compact dual-band bandpass filter (BPF) using two stub-loaded stepped impedance resonators (SLSIRs) is proposed in [3]. A compact dual-band BPF operating at 1.27 GHz for GPS-L2 application, and 2.45 GHz for WLAN application is designed and fabricated by using two SLSIRs. This compact filter has mixed electrical and magnetic coupling between two SLSIRs to produce multiple transmission zeros located on either side of each passband. To achieve dual-band filter, planar cross-coupled filters with a dual-passband quasi- elliptic function response are presented in [4]. The author has employed two different hairpin resonators to determine the proper couplings necessary for the two design frequencies. A compact dual-mode dual-band microstrip bandpass filter with a different feeding scheme has been introduced in [5]. The proposed filter

has been also designed by locating the one resonator within the other to reduce size of the circuit.

In this paper, the microstrip dual-band filter design is presented. The filter consists of folded open-circuited stubs with slow wave effect and a connecting line between the folded stubs. The slow wave effect is provided by interdigital unit cells in order to create a capacitive effect. Also, a slit is placed in the middle of the connecting line to control the return loss level in each passband, sensitively. Adding vias to the resonator allows to achieve lower passband and transform from lowpass to bandpass characteristic in the first band. It has been shown that the proposed dual-band filter has a significant feature that remove the extra surface area.

II. The Proposed Resonator with Slow Wave Effect

The microstrip open loop resonator is investigated to design of the dual-band bandpass filter circuit, in this section. The resonator consists of two pairs of open circuited stubs and connecting line between these stubs, as illustrated in Fig. 1a. I/O ports are directly connected to open loop resonator. As can be seen from the figure, the connecting line and open circuited stubs are configured with different widths. Thus, the proposed resonator is not only more compact than conventional stub-loaded filters, but also more miniature in size, as described in [6]. It is quite important in terms of size reduction. The equivalent circuit for the proposed resonator is also given in Fig. lc. To perform the even-odd mode analysis, the circuit is divided into two parts along the symmetry axis and equivalent half circuit is ended as short/open circuit for odd/ even mode excitation, respectively. For odd/even mode excitation, the input admittance of the circuit is expressed as,

$$Y_{even/odd} = Y_1 + Y_2 + Y_3 \tag{1}$$

where Y_1, Y_2 and Y_3 are admittances seen from input of each line. It can be written as Y_1=Y_3 since the open-circuited stubs at the bottom and upper side are equal, as can be seen from Fig. 2a/2b. These admittances can be calculated as given in (2)-(3) for even mode excitation and (4)-(5) for odd mode excitation. In (2)-(5), Y_{0i} and θ_i are the characteristic admittance and electrical length of the related line. Also, Y_p and Y_g indicate the admittance of shunt and series capacitor, which are used to represent the equivalent circuit of the gap, respectively. For demonstration the theory, the calculated and simulated frequency response is compared in Fig. 2c. The circuit is configurated on an RT/Duroid 5880 substrate with a relative permittivity of ε_r = 2.2 and thickness of h = 0.51 mm. The resonator dimensions are w_1 = 2.0 mm, w_2 = 3.0 mm, w_3 = 1.6 mm and g = 0.6 mm.

In order to achieve more significantly miniaturization and compactness as compared to the resonator as given in Fig. 1a, the interdigital unit cells are located in the resonator having same surface area as illustrated in Fig.1b. The interdigital structure consists of periodic multi-fingers with equal gaps. As well, the mutual interdigital fingers have same length. The interdigital structure is short-circuited on one side of the conductor by means of metal vias in order to create capacitive loading effect. It is denoted as C_{int} in the equivalent circuit model given in Fig. 1b. The metal vias are located in the middle of the conductor and distance between the metal vias is chosen to be equal. The interdigital unit cells use the capacitance that arise from the gap between conductors. The layout of the resonator loaded interdigital capacitance is given in Fig. 1b. By adding interdigital unit cells to the resonator and increasing the length of the interdigital fingers, the capacitance per unit length increases while the inductance per unit length is approximately kept. In this case, propagation velocity is reduced and the slow wave effect (SWE) is achieved successfully. Thus, the resonance frequency is expected to shift down as the number (n) and the length (l_i) of the interdigital unit cells increases, in the proposed resonator.

Both resonators have been simulated by using a full wave electromagnetic simulator to observe the slow wave effect [7]. The simulated frequency response of the resonators with/without interdigital unit cells can be seen in Fig. 2d. Frequency response is obtained when 0.5 mm wide interdigital fingers are placed at 0.5 mm intervals on the circuit with the same surface area as the resonator circuit given in Fig 1b. In this case, the resonance frequency is reduced about 600 MHz by means of interdigital unit cells. Thus, the proposed resonator has compact size due to interdigital unit cells and it can be reduced size as compared conventional stub loaded resonator, significantly. It is obvious that, the proposed resonator configuration is quite suitable for miniaturizing.

The interdigital unit cells not only provide compact size but also ensure controlling the mode frequencies, sensitively. The capacitive loading of the resonator arms increases/decreases when the length of the interdigital fingers

$$Y_1 = Y_3 = Y_{02}\frac{Y_{01}Y_p - Y_{02}Y_p \tan\theta_1 \tan\theta_2 + jY_{01}^2 \tan\theta_1 + j\,Y_{01}Y_{02}\tan\theta_2}{Y_{01}Y_{02} - Y_{01}^2 \tan\theta_1 \tan\theta_2 + jY_{01}Y_p \tan\theta_2 + jY_{02}Y_p \tan\theta_1} \tag{2}$$

$$Y_2 = jY_{03}\tan\left(\frac{\theta_3}{2}\right) \tag{3}$$

$$Y_1 = Y_3 = Y_{02}\frac{Y_{01}Y_g + Y_{01}Y_p - Y_{02}Y_g \tan\theta_1 \tan\theta_2 - Y_{02}Y_p \tan\theta_1 \tan\theta_2 + jY_{01}^2 \tan\theta_1 + j\tan\theta_2 Y_{01}Y_{02}}{Y_{02}[Y_{01} + j(Y_g + Y_p)\tan\theta_1] + jY_{01}\tan\theta_2[jY_{01}\tan\theta_1 + Y_g + Y_p]} \tag{4}$$

$$Y_2 = -jY_{03}\cot\left(\frac{\theta_3}{2}\right) \tag{5}$$

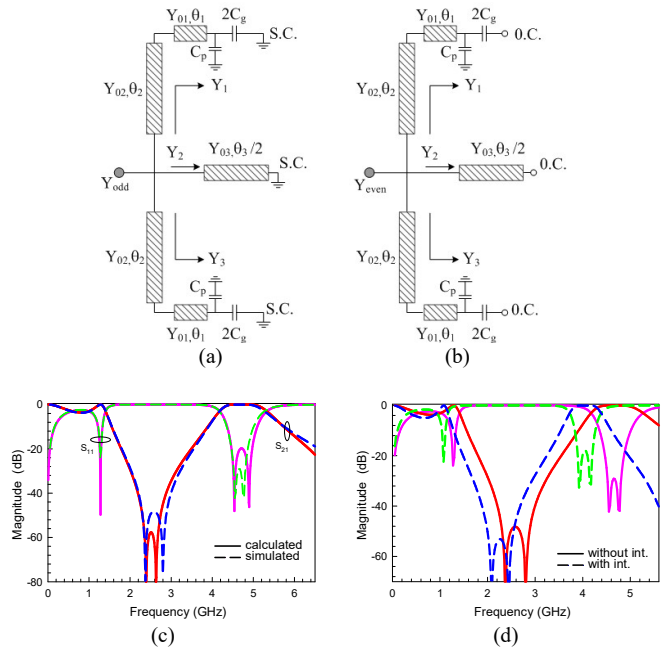

Fig. 2. Equivalent circuit for (a) odd mode; (b) even mode extraction; comparison of the (c) calculated and simulated responses; (d) without and with interdigital unit cell.

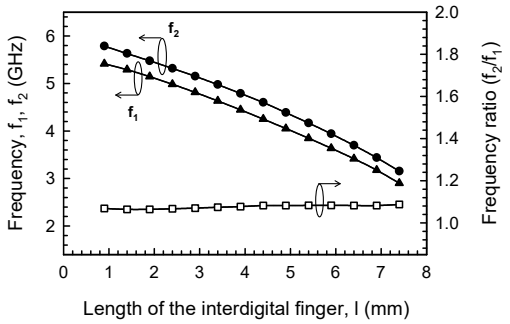

Fig. 3. Simulated mode frequencies of resonator with interdigital loading

is increased/decreased, these changes affect mode frequencies in each passband and transmission zeros. For instance, the change of the mode frequencies (f_1 and f_2) at the second passband depending on the different lengths of the interdigital fingers can be clearly observed in Fig. 3. The mode frequencies at second passband decrease as the length of the interdigital fingers increases. Also, the ratio of the mode frequencies (f_2/f_1) can be calculated as a function versus the length of the interdigital fingers. It is possible to observe that the ratio remained almost fixed from the graph.

III. Dual Band Filter Design

A novel compact dual-mode dual-band bandpass filter using the resonator topology detailed in the previous section is illustrated in Fig. 4. To perform a filter with a dual-passband response, metal vias connecting the stubs to the ground plane are used on the open circuited stubs. It is observed that by adding vias to each open-circuited stubs, a lower passband is created in the frequency response. In this case, a design proposal is presented to remove the extra surface area. Several attractive approaches have been used to achieve dual-band

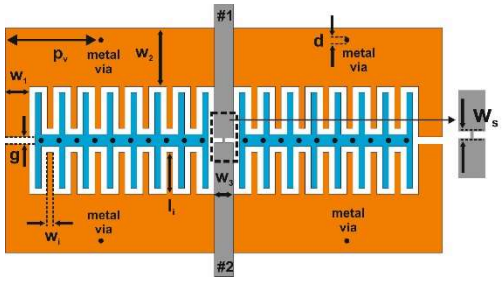

Fig. 4. Configuration of the dual-mode dual-band bandpass filter.

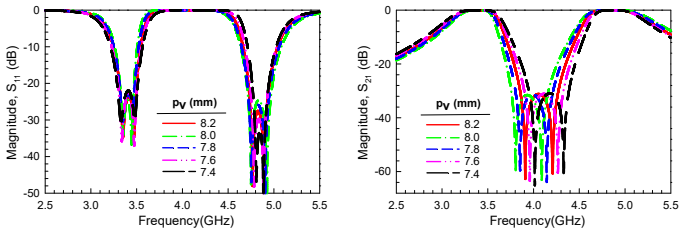

Fig. 5. Simulated frequency response for different p_v (a) S_{11}; (b) S_{21}.

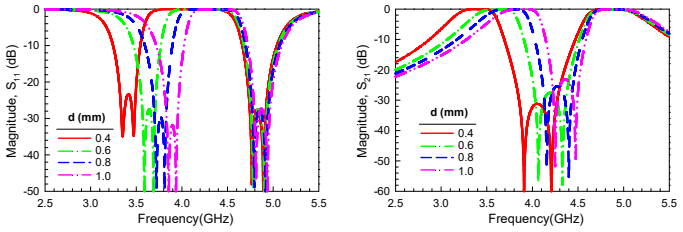

Fig. 6. Simulated frequency response for different d (a) S_{11}; (b) S_{21}.

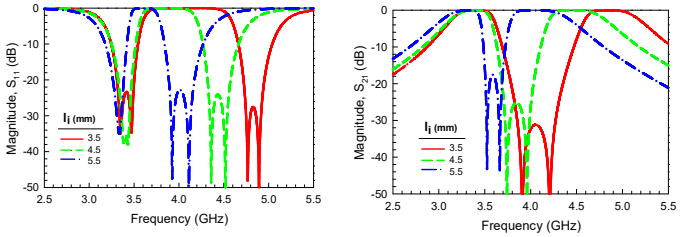

Fig. 7. Simulated frequency response versus l_i (a) S_{11}; (b) S_{21}.

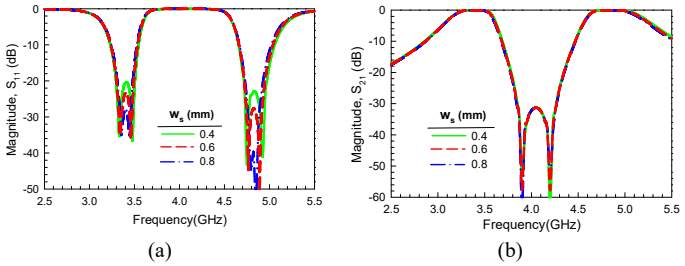

Fig. 8. Simulated frequency response versus w_s (a) S_{11}; (b) S_{21}.

filters, such as a stepped impedance resonator, stub-loaded resonator, or coupled lines but these structures need larger circuit size due to the use of multiple resonators. In this paper, the most important feature of the proposed configuration for a dual-band filter design is that the circuit can occur in the surface area of a single resonator without any extra area.

Some implementations for the effect of the design parameters on the frequency response are also investigated in this section. The position of the vias (p_v) placed on the open circuited stubs can be used to control the transmission zeros. Fig. 5 shows variation of the in-band return loss levels each passband and transmission zeros according to p_v value. While the return loss level in each passband is kept fixed, transmission zeros change. Thus, transmission zeros can easily be controlled independently from the other mode frequencies. The return loss level of the first passband is not affected by diameter of the vias (d), as depicted in Fig. 6. By variation d, the return loss level of the first passband is kept at almost the same level, but the return loss of the second passband can be changed quickly. The length of the interdigital fingers (l_i) can be used to affect only the second passband and the position of the transmission zeros, as illustrated in Fig.7. By increasing the length of the capacitive fingers, the slow wave effect is increased and it is allowed that the center frequency of the second passband is shifted down. And also, the mode frequencies of the first passband are almost fixed. All these observations show that each passband can easily be controlled independently from the other one. Additionally, a slit is placed on the connecting line between the open-circuited stubs, as can be shown from Fig. 4. The width of the slit is called w_s and the effects of the width on the frequency response are represented in Fig. 8. Return loss level of each passband can be controlled against w_s, simultaneously. The total surface area is 22.8 mm x 36.6 mm in all simulation.

IV. Experimental Study

To demonstrate the proposed approach, dual-band bandpass filter has been designed and fabricated on an RT/Duroid 5880 substrate with a thickness of 0.51 mm and a relative dielectric constant of 2.2. Photograph of the fabricated filter is shown in Fig. 9a. The overall size of the designed filter is about 0.392 λ_g x 0.63 λ_g. λ_g is the guided wavelength at measured center frequency of first passband. All physical dimensions of the filter are given in Table I. Measurement has been performed by a Vector Network Analyzer Keysight N5222A PNA. The comparison of the measured and simulated results is depicted in Fig. 9b. According to measured results, the measured in-band return losses for the first/second passbands are 20.01/18.05 dB, the measured insertion losses at center frequencies are 0.64 and 0.95 dB, respectively. The measured and simulated results exhibit a good agreement.

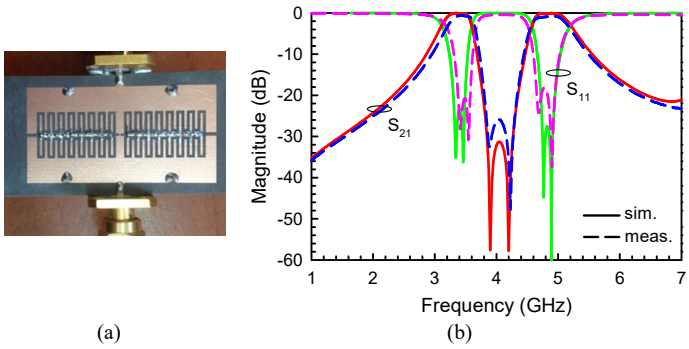

(a) (b)

Fig. 9. (a) Photograph of fabricated circuit; (b) comparison of the simulated and measured results.

Table 1. Dimensions of the fabricated circuit (All units are in mm.).

Parameters	w_1	w_2	w_3	w_i	l_i	p_v	g	d
Dimensions	2.0	4.9	1.6	0.5	3.5	7.8	0.6	0.4

V. Conclusion

The theory and experiment of microstrip resonators with two pair of open-circuited stub have been presented. The proposed resonator is directly connected to I/O ports to obtain a wideband frequency response. In addition, the resonator has become a more compact circuit with capacitively loaded through interdigital unit cells. The capacitive loading has allowed observing the slow wave effect. Dual-band response is achieved by using metal vias in open-circuited stubs. In this way, it is possible to achieve the second passband without the need for an extra resonator circuit, using the same surface area where the single passband response is obtained. The dual-band filter design parameters have been described in detail by using a full wave electromagnetic simulator. It is obvious that the proposed filter has not only a compact size due to the slow-wave effect but also a miniature size in terms of surface area. To verify the validity of the circuit, a dual-band bandpass filter prototype has been fabricated, tested and discussed the experimental results. The results show a good agreement.

Acknowledgment

This work was supported by the Scientific and Technological Research Council of Turkey (TUBITAK) under Grant 120E101.

References

[1] N. Han, Y. Dong and M. Wang, "A dual-band bandpass filter using parallel doubly coupled structure with loading capacitance," *2010 International Conference on Microwave and Millimeter Wave Technology*, 2010, pp. 1849-1851.

[2] Sheng Sun and Lei Zhu, "Compact dual-band microstrip bandpass filter without external feeds," *IEEE Microwave and Wireless Components Letters*, vol. 15, no. 10, pp. 644-646, Oct. 2005.

[3] P. Wen, Z. Ma, H. Liu, M. Ohira, B. Ren and X. Wang, "Compact dual-band bandpass filter using stub-loaded stepped impedance resonators with mixed electric and magnetic couplings," *2017 IEEE Asia Pacific Microwave Conference (APMC)*, 2017, pp. 803-805.

[4] J.-T. Kuo and H.-S. Cheng, "Design of quasi-elliptic function filters with a dual-passband response," *IEEE Microwave and Wireless Components Letters*, vol. 14, no. 10, pp. 472-474, Oct. 2004.

[5] C. Karpuz and A.K. Gorur, "A novel compact configuration for dual-mode microstrip resonators and dual-band bandpass filter applications," Microwave and Optical Technology Letters, vol. 55, no. 4, pp. 775-779, April, 2013.

[6] A. Gorur and C. Karpuz, "Reduced-size wideband bandstop filter using two open-circuited shunt stubs spaced by a double-length transmission-line element," *International Journal of RF and Microwave Computer-Aided Engineering*, vol. 15, no. 1, pp. 79-85, Jan. 2005.

[7] Sonnet User's Manual, Version 16, Sonnet Software, North Syracuse, NY, June 2016.